Supporting information for

Near Unity Absorption in Nanocrystal Based Short Wave Infrared Photodetectors using Guided Mode Resonators

Audrey Chu[1,2], Charlie Gréboval[1], Nicolas Goubet[1,3], Bertille Martinez[1], Clément Livache[1,5], Junling Qu[1], Prachi Rastogi[1], Francesco Andrea Bresciani[1], Yoann Prado[1], Stephan Suffit[4], Sandrine Ithurria[5], Gregory Vincent[2]*, Emmanuel Lhuillier[1]*

[1]Sorbonne Université, CNRS, Institut des NanoSciences de Paris, INSP, F-75005 Paris, France

[2] ONERA -The French Aerospace Lab, 6, chemin de la Vauve aux Granges, BP 80100, F-91123 Palaiseau, France

[3]Sorbonne Université, CNRS, De la Molécule aux Nano-objets: Réactivité, Interactions et Spectroscopies, MONARIS, F-75005 Paris, France

[4]Laboratoire Matériaux et Phénomènes Quantiques, UMR 7162 CNRS, Université Paris Diderot, Paris, France

[5]Laboratoire de Physique et d'Etude des Matériaux, ESPCI-ParisTech, PSL Research University, Sorbonne Université UPMC Univ Paris 06, CNRS, 10 rue Vauquelin 75005 Paris, France.

To whom correspondence should be sent: el@insp.upmc.fr and gregory.vincent@onera.fr

Table of contents

1. Device preparation

1.1. Electrodes Fabrications

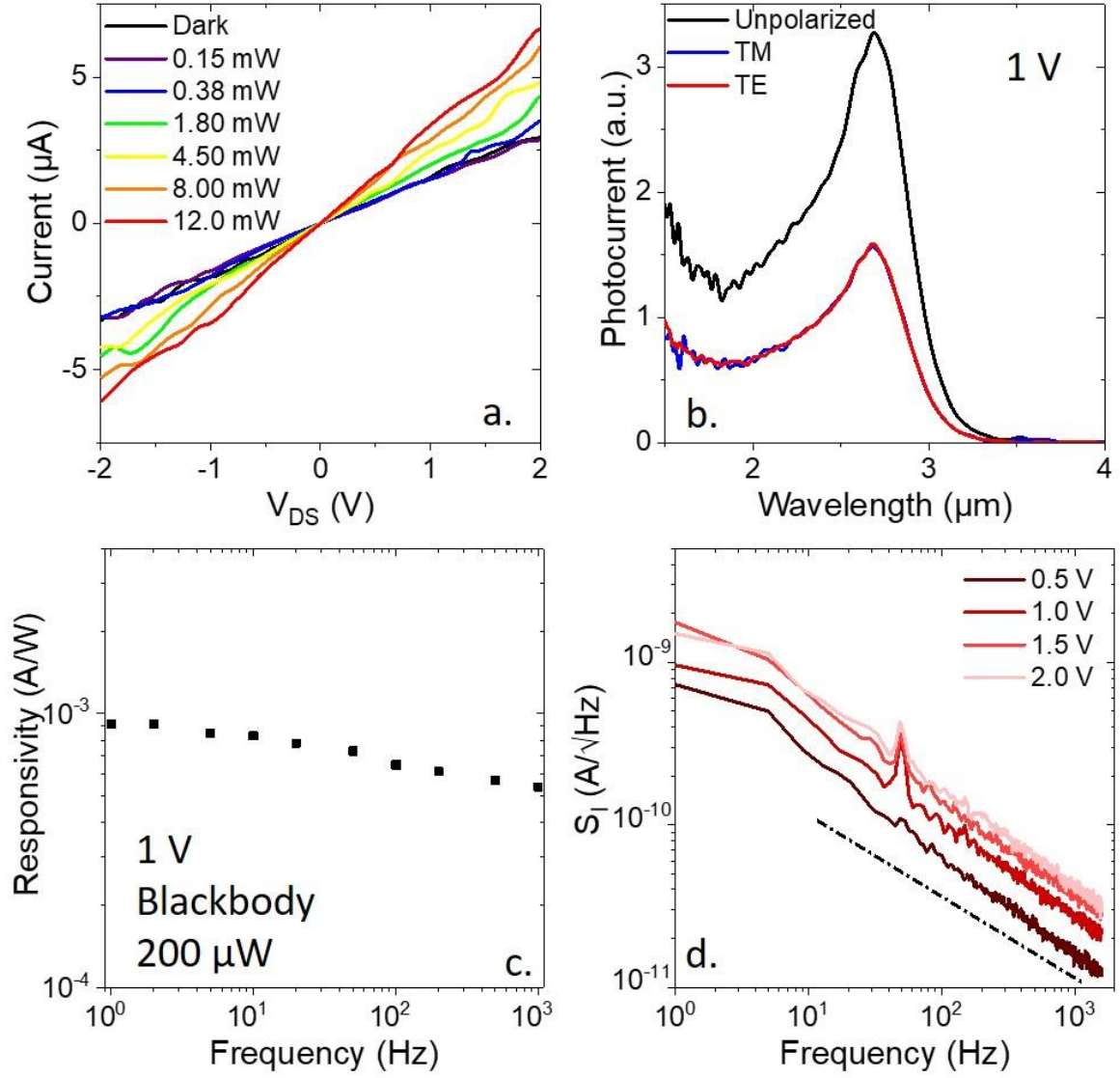*Interdigitated Electrodes*. The surface of Si/SiO$_2$ wafer (400 nm oxide layer) is cleaned by sonication in acetone. The wafer is rinsed with acetone, then isopropanol and dried with a N$_2$ gun. A final cleaning is made using an O$_2$ plasma. An adhesion promoter (TI PRIME) is spin-coated onto the substrate and baked at 120 °C for 2 min. AZ5214E is spin-coated and baked at 110 °C for 90 s. The substrate is exposed under UV through a pattern mask for 1.5 s. The film is then baked at 125 °C for 2 min in order to invert the resist. Then a 40 s flood exposure is performed. The resist is developed using a bath of AZ726 for 25 s, rinsed in pure water and dried with N$_2$. We then deposit 5 nm of chromium and 80 nm of gold using thermal evaporation. The lift-off is performed by dipping the film in acetone for 1 hour. The electrodes are rinsed using isopropanol and dried using a N$_2$ gun. The electrodes are 2.5 mm long, 10 µm large and spaced by 20 µm. In the main article, they are called "conventional electrodes", in contrast to nanoelectrodes used to induce GMR.

The performances of devices based on such 30 µm period interdigitated electrodes are given respectively for PbS in **Figure S 1** and for HgTe in **Figure S 2**. In this case the ligand exchange is performed to make the film conductive by using ethanedithiol.

Figure S 1 PbS nanocrystals on 30 µm period interdigitated electrode : *a. I-V curves under dark condition and under illumination (λ=1.55 µm) measured at room temperature under various incident laser powers. b. Photocurrent spectra of the device for TE (red) and TM (blue) modes, as well as the total (black) photocurrent. c. Responsivity at 1 V as a function of the signal frequency. d. Noise current spectral density as a function of the signal frequency. Dash line corresponds to 1/f noise decay.*

Figure S 2 HgTe nanocrystals on 30 µm period interdigitated electrode *: a. I-V curves under dark condition and under illumination (λ=1.55 µm) measured at room temperature under various incident laser power. b. Photocurrent spectra of the device for the TE (red) and TM (blue) mode, as well as the total (black) photocurrent. c. Responsivity at 1 V as a function of the signal frequency. d. Noise current spectral density as a function of the signal frequency. Dash line corresponds to 1/f noise decay.*

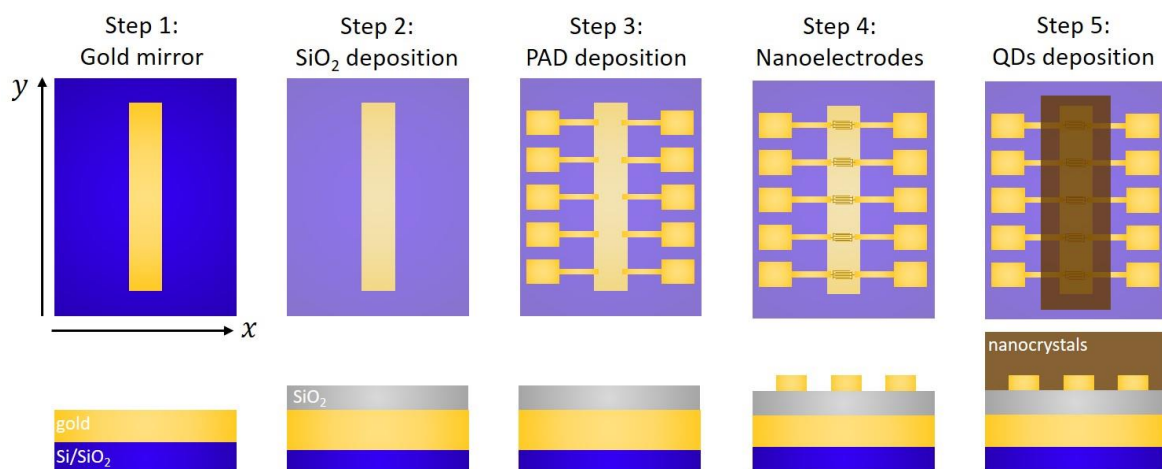### 1.2. Fabrication of the electrodes used to induce a GMR

<u>Step 1: Deposition of the gold mirror.</u> The surface of Si/SiO$_2$ wafer (400 nm oxide layer) is cleaned by sonication in acetone. The wafer is rinsed with acetone, then isopropanol and dried with a N$_2$ gun. A final cleaning is made using an O$_2$ plasma. An adhesion promoter (TI PRIME) is spin-coated onto the substrate and baked at 120 °C for 2 min. AZ5214E is spin-coated and baked at 110 °C for 90 s. The substrate is exposed under UV through a pattern mask for 1.5 s. The film is then baked at 125 °C for 2 min in order to invert the resist. Then a 40 s flood exposure is performed. The resist is developed using a bath of AZ726 for 32 s, rinsed in pure water and finally dried with N$_2$. We then deposit 5 nm of chromium and 80 nm of gold using thermal evaporation. The lift-off is performed by dipping the film in acetone for 1 hour. The gold mirror is rinsed using isopropanol and dried with a N$_2$ flow.

<u>Step 2: Insulating gold mirror.</u> The samples patterned with the gold mirror are put in an Alcatel sputtering chamber for a 45 min deposition of SiOx, at 120 W. At the end of sputtering, the obtained SiOx layer is 120 nm thick.

<u>Step 3 Deposition of macroscopic pads for reporting electric contacts.</u> After having rinsed the sample with acetone and isopropanol, the adhesion promoter and the resist are deposited as described in step 1. The sample is then exposed through a second chromium mask for 1.5 s. The same resist inversion process as described in step 1 (annealing + flood exposure) is performed before developing the sample in AZ726 developer for 25 s and rinsing it in pure water. The patterned sample is then introduced into a VINCI evaporator for deposition of 5 nm of Chromium and 150 nm of gold. At the end, the sample is dipped in acetone overnight to remove remaining resist.

<u>Step 4 Deposition of nanoelectrodes.</u> After having rinsed the sample with acetone and isopropanol, a layer of A6 PMMA 950 is spin-coated onto the substrate and baked for 15 min at 150 °C. The samples are transferred in a Zeiss Supra 40 SEM with Raith ELPHYS Quantum device for electron beam lithography. The operating bias is set to 20 kV and the aperture to 15 µm. The current is measured at 70 pA. The dose is set at 220 µC.cm^{-2}. The PMMA is developed by dipping the film in a solution of MIBK:isopropanol (1:3) for 50 s and rinsed in pure isopropanol for 20 s. We then deposit a 5 nm layer of chromium and a 50 nm layer of gold using thermal evaporation. The lift-off is performed by dipping the film in acetone overnight. Sonication at low power is necessary to remove the remaining resist. 20 pairs of digits are deposited as electrodes. The electrodes are 500 µm long. For a resonance at 1.5 µm the digits are 350 nm wide and separated by 750 nm. For a 2.5 µm resonance, the digits are 900 nm wide and separated by 900 nm.

The **Figure S 3** is a schematic of these main fabrication steps.

| Step 1: | Step 2: | Step 3: | Step 4: | Step 5: |
| Gold mirror | SiO$_2$ deposition | PAD deposition | Nanoelectrodes | QDs deposition |

Figure S 3 Main fabrication steps of the electrodes used to induce a GMR. Top part is a top view, while bottom part is a side view. Step one relates to the deposition of the gold mirror. Step 2 relates to the deposistion of SiO₂ dielectric to avoid shorts through the back mirror. Step 3 relates to the deposition of the macroscopic pads. Step 4 relates to the fabrication of the interdigitated electrodes inducing GMR, thanks to e-beam lithography. Step 5 relates to the CQD film deposition.

1.3. Thin film deposition

Solid state ligand exchange. CQD solutions (PbS or HgTe in toluene) are diluted at 30 mg.mL^{-1}. In a N$_2$-filled glovebox, this solution is spin-coated onto the substrate at 2000 rpm for 60 s. The film is then dipped in a solution of new ligands for 45 s. Typically the ligand exchange solution is an EDT solution at 1 wt% in ethanol. The film is then rinsed in pure ethanol for 20 s. This process is repeated in order to reach the targeted thickness (200 nm). For 200 nm of PbS, this process is repeated 10 times. Note, that there is no encapsulation layer on the top of the device.

2. Electromagnetic simulation

Calculations have been achieved with Matlab library based on Rigorous Coupled-Wave Analysis[1] (RCWA). We considered incoming plane wave under normal incidence, either with transverse magnetic (TM) or transverse electric (TE) polarization, i.e. with magnetic field or electric field parallel with the slits of the gratings, respectively. Grating is supposed to be invariant along *y* direction, and repeated infinitely along *x* direction.

2.1. Inputs for simulation

For each device (PbS or HgTe), the layers are given in Table S 1.

Table S 1: Layer thicknesses for each stack

Layer	Interdigitated on Au/SiO₂ for GMR	Interdigitated on Au/SiO₂ for GMR
External environment	Air	Air
Film	PbS (200 nm)	HgTe (220 nm)
Structure	PbS/Au (750/350 nm) t_g=50 nm	HgTe/Au (900/900 nm) t_g=50 nm
Dielectric	120 nm	120 nm
Gold mirror	200 nm	200 nm

The last input needed for these calculations is the complex refractive index of each layer. For the gold[2] we used previously reported refractive indices. For the SiO₂, we use n=1.44 and k=0, and n=1 for the air.

For the real part of the nanocrystal film refractive index, we used the value of 2 which is commonly used for nanocrystal thin film. For the imaginary part we used the shape of the absorption feature. In the case of PbS we calculated Im(n) at the band edge using Moreel's paper [3] to give an absolute value. Using (1) and (2) it is possible to calculate the absorption coefficient at the band edge and to deduce the Im(n) at that point using (3).

$$(1) \qquad E_0 = \frac{1}{0.016d^2 + 0.209d + 0.45}$$

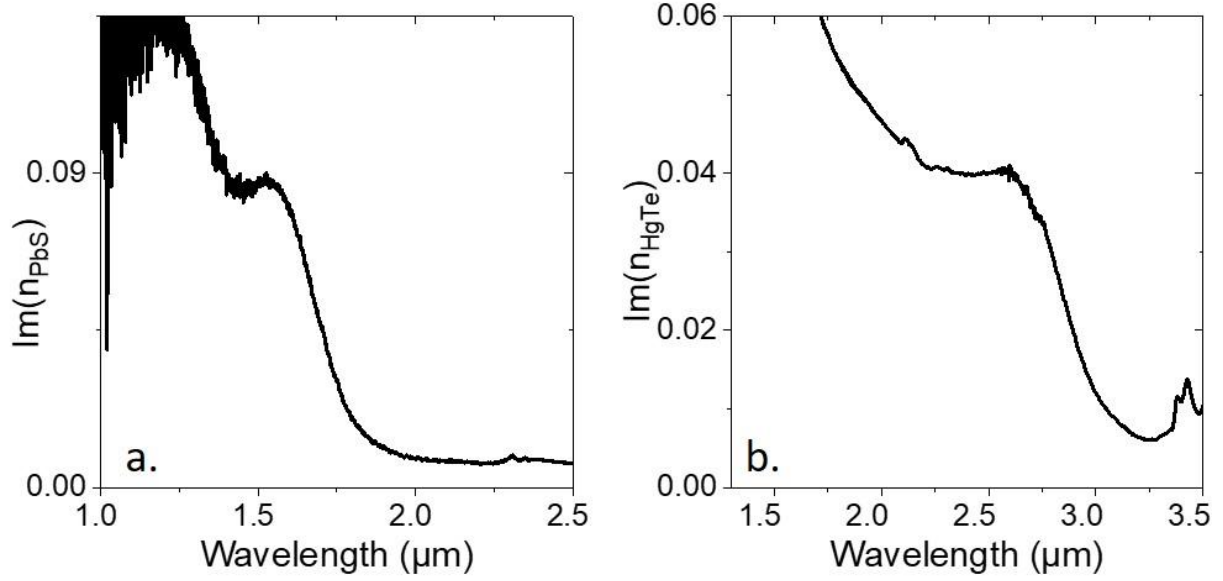$$(2) \qquad \mu = \frac{1.85 * 10}{d^2} \ (cm^{-1}.meV)$$

Where E_0 is the band edge energy, d the particle diameter and μ the integrated absorption coefficient.

$$(3) \qquad k = \frac{\alpha\lambda}{4\pi}$$

With $k = Im(\underline{n})$, λ is the wavelength and α is the absorption coefficient (cm⁻¹).

Using those formula, we calculated Im(n)=0.09 at the band edge. The wavelength dependence of k is given in **Figure S 4**a.

For HgTe, the absorption coefficient is measured to be 3×10^3 cm^{-1} which give k=0.04 at the band edge. The wavelength dependence of k is given in **Figure S 4**b.

Figure S 4 Refractive indices used for simulation. *a. Imaginary part of n for PbS 6k used in the study. b. Imaginary part of n for the HgTe 4k used in the study.*

The absorption map is deduced from the electric field at each point:

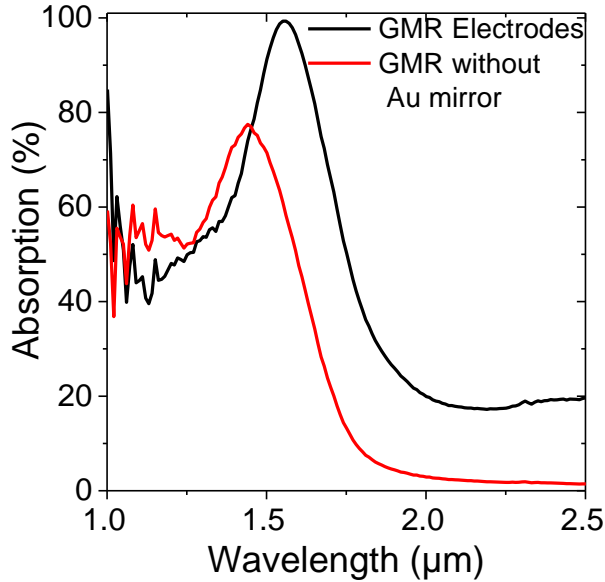$$Absorption = \frac{\pi}{\lambda} \int_S Im(\varepsilon(M))(|E_y|^2)dS, \qquad in\ TE\ polarisation$$

$$Absorption = \frac{\pi}{\lambda} \int_S Im(\varepsilon(M))(|E_x|^2 + |E_z|^2)dS, \qquad in\ TM\ polarisation$$

Where S is a surface, $\varepsilon(M)$ is the permittivity at a point $M(x, y, z)$.
In the code the losses are calculated at each point of the map.

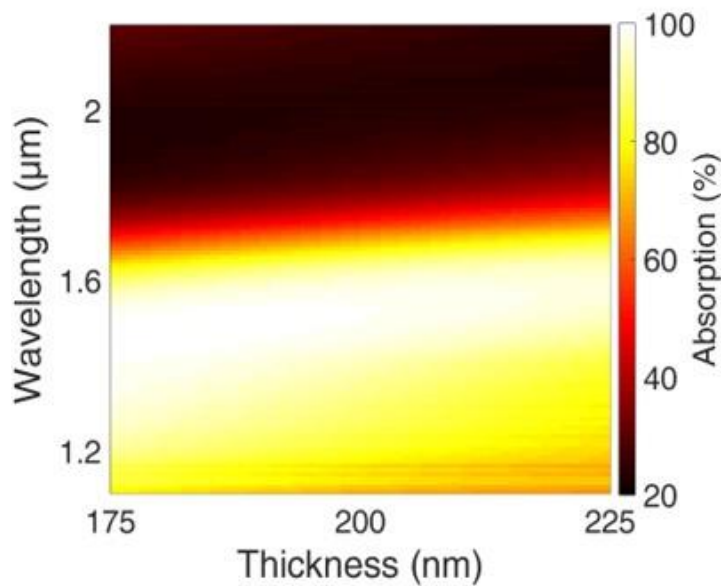## 2.3. Effect of the back-side gold mirror

In **Figure S 5**, the effect of the gold mirror is shown. The GMR resonance is due to the grating and should not be too affected by the back-side gold mirror. Even without the gold mirror a strong resonance is effectively present. However, the absorbance is lower due to a partial transmission.
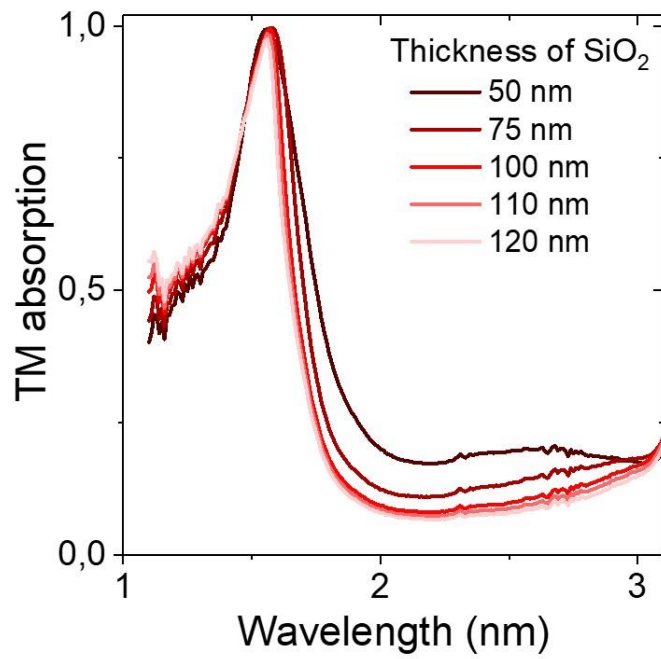

Figure S 5 Effect of back-side gold mirror. *Simulated absorption spectra of the TM component of the CQD film grafted with GMR electrodes with or without the back-side gold mirror. Simulations are conducted using PbS 6k.*

2.2. Effect of film thickness and surface topology

To consider the robustness of the proposed device toward deviation of geometrical factors (change of pattern size during lithography and CQD film roughness) we have quantized how the TM spectrum is affected by the film thickness in **Figure S 6** and by the change of the dielectric thickness, see **Figure S 7**.
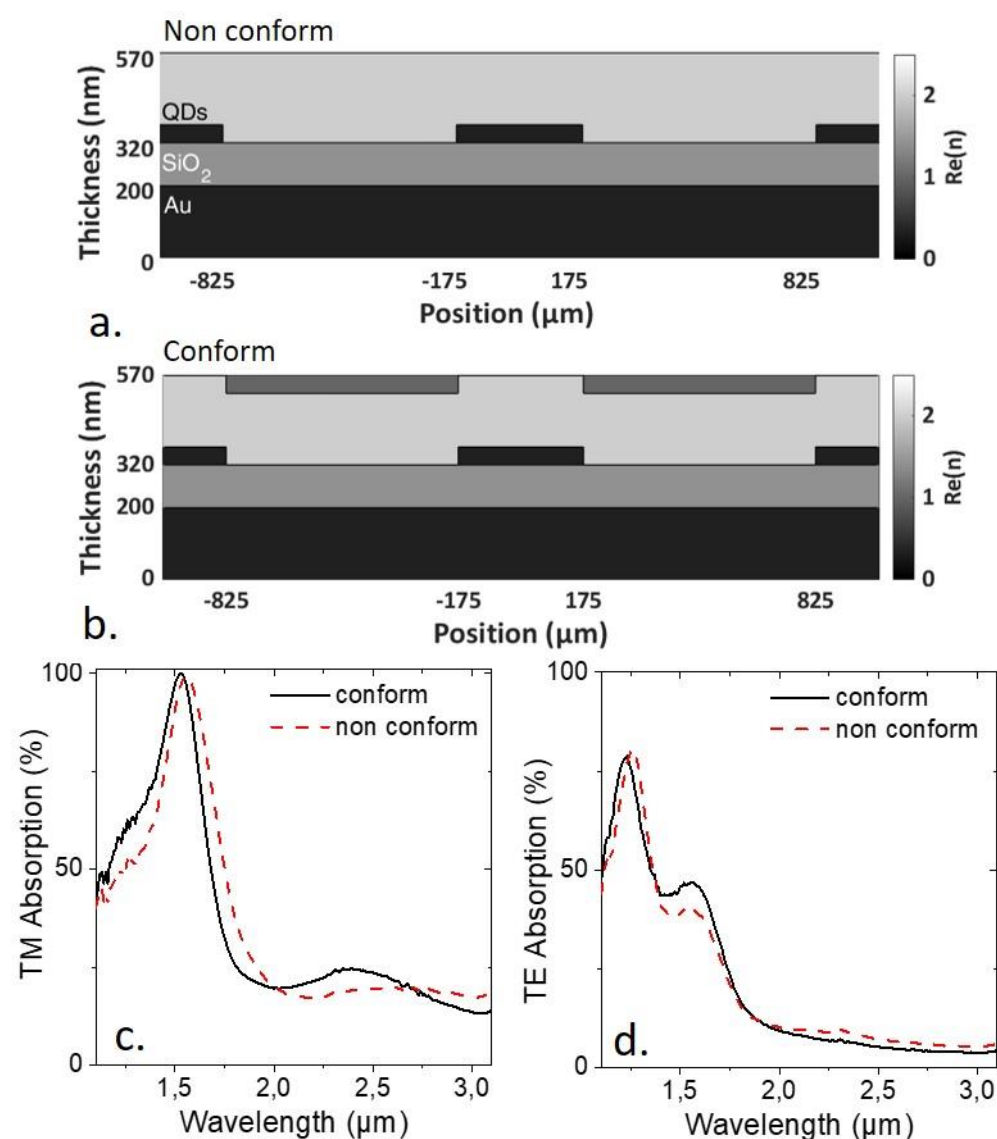

Figure S 6 Effect of film thickness for PbS CQD based device. Absorption spectrum as a function of the film thickness.
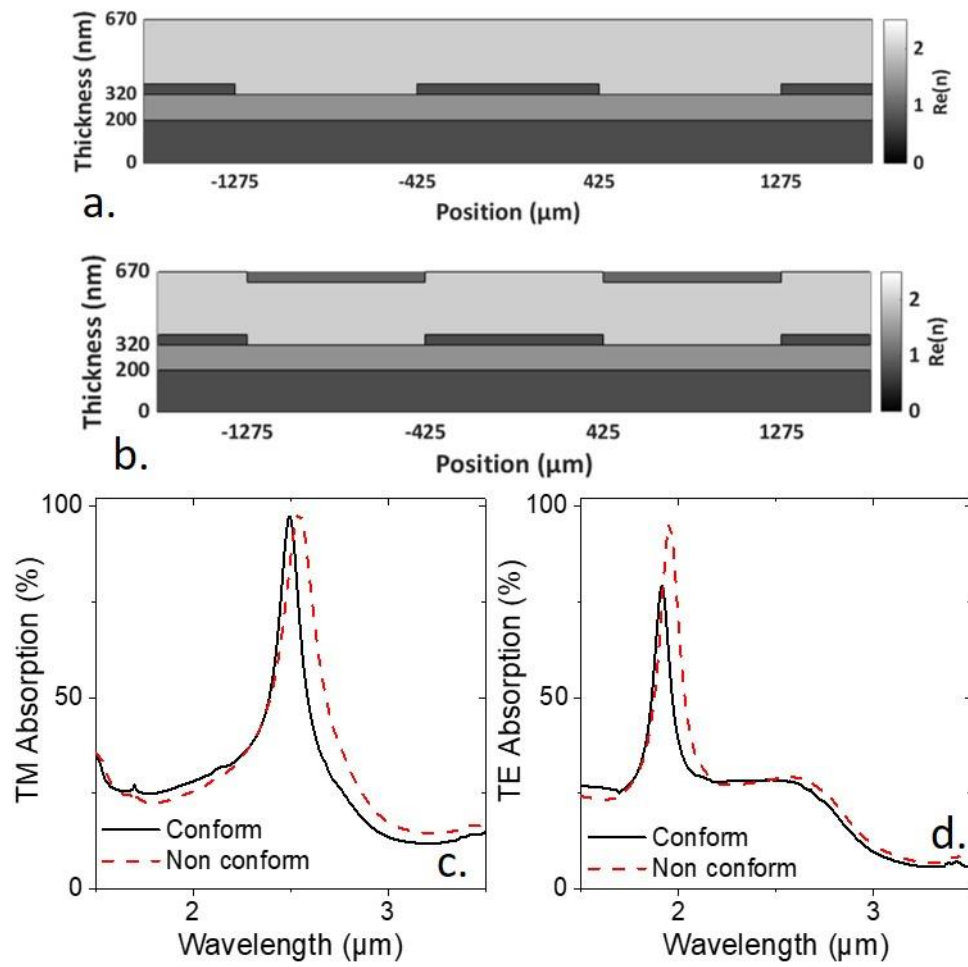
Figure S 7 Effect of dielectric thickness. *Absorption spectra relative to the TM mode for the PbS CQD-based device for different thicknesses of the dielectric layer.*

This GMR geometry is compatible with relatively thick layer of dielectric which is convenient to prevent electrical short though the back-side mirror.

We have also quantized how the spectra relative to the TE and TM modes are affected by the conformity of the film deposition. The result for the device based on PbS and HgTe nanocrystals are respectively given in **Figure S 8** and **Figure S 9**.
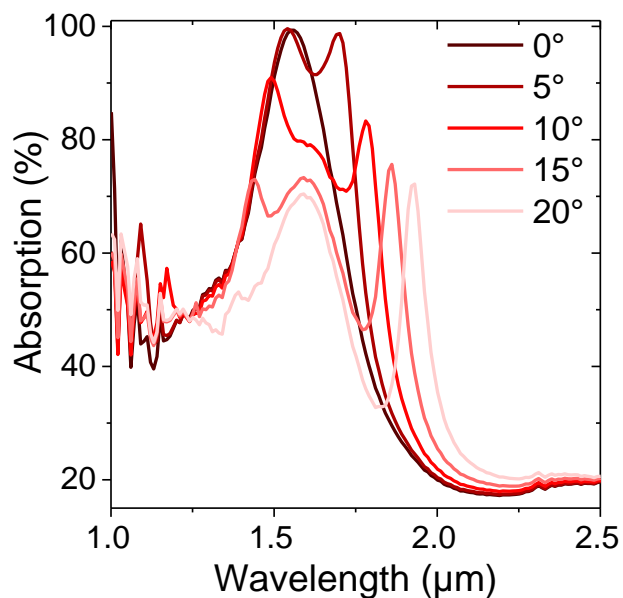

***Figure S 8 Effect of conformity for PbS CQD based device**. A diagram of the device when the CQD film is non-conformed (a) and conformed (b). c. Absorption spectra relative to the TM mode. d. Absorption spectra relative to the TE mode.*

Figure S 9 Effect of conformity for HgTe CQD based device. *A diagram of the device when the CQD film is non-conformed (a) and conformed (b). c. Absorption spectra relative to the TM mode. d. Absorption spectra relative to the TE mode.*
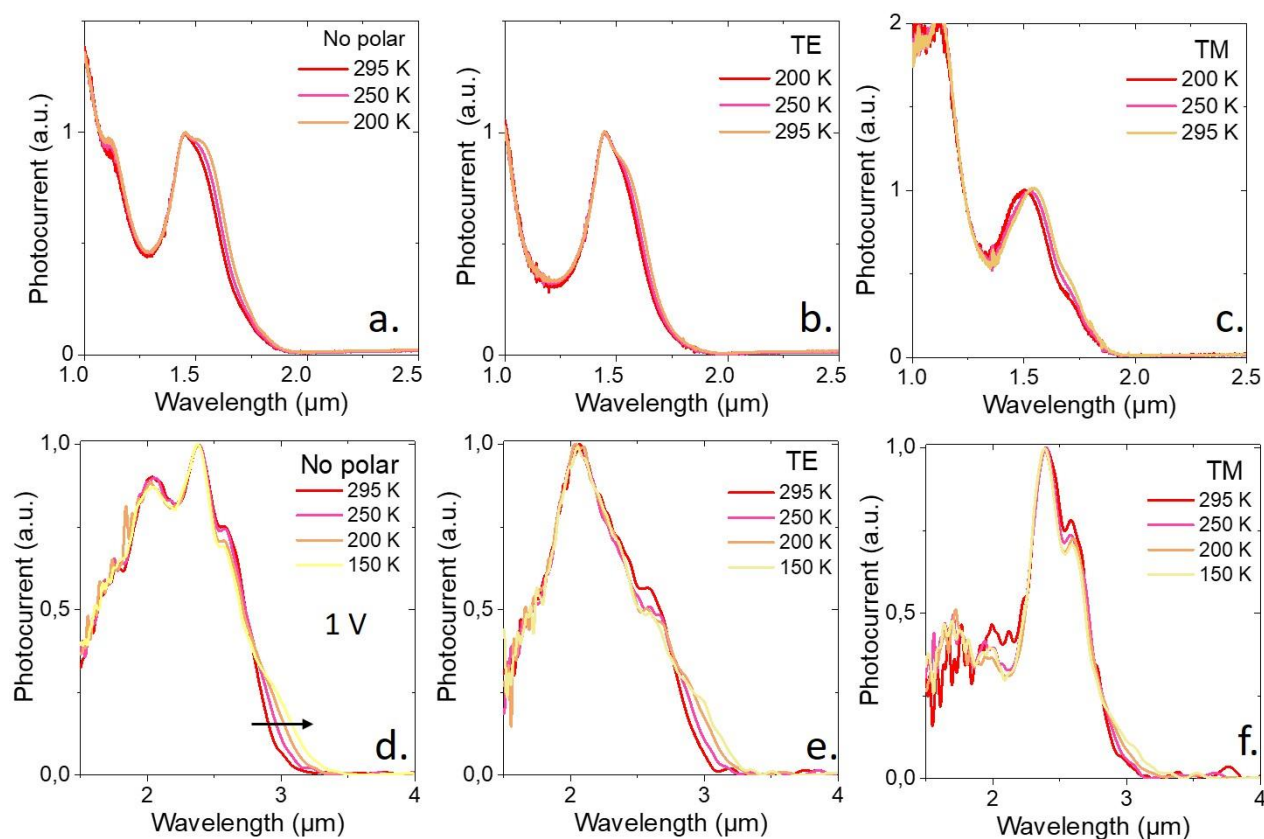
2.4. Effect of the incident angle

The structure is dispersive. The effect of the incident angle is given **Figure S 10**. The absorption peak is split in two by the addition of a small angle (5° typically). In other words, exciton and GMR are no longer spectrally matched. The GMR peak then redshifts with the increase of the angle.

Figure S 10 Effect of the incident-light angle on the absorption spectra. *Simulated absorption spectra of the TM component of the CQD film grafted with GMR electrodes at different angles of the incident light. The simulations are conducted using PbS 6k.*

3. Effect of temperature

We have measured the photocurrent spectra for the PbS and HgTe based device. In both cases, we observed a redshift of the material band-edge as the sample are cooled down. This is the expected temperature dependence for PbS[4] and HgTe[5]. On the other hand, the peaks resulting from resonance do not shift with temperature, see **Figure S 11**.

Figure S 11 Effect of temperature on the photocurrent spectra. Photocurrent spectra of the PbS device at three temperatures relative to the total signal (a.), TE mode (b.) and TM mode (c.). Photocurrent spectra of the HgTe device at four temperatures relative to the total signal (d.), TE mode (e.) and TM mode (f).

4. REFERENCES

(1)   Hugonin, J.-P.; Lalanne, P. Reticolo Software for Grating Analysis. Reticolo software for grating analysis, Institut d'Optique, Orsay, France 2005.

(2)   Olmon, R. L.; Slovick, B.; Johnson, T. W.; Shelton, D.; Oh, S.-H.; Boreman, G. D.; Raschke, M. B. Optical Dielectric Function of Gold. *Phys. Rev. B* **2012**, *86*, 235147.

(3)   Moreels, I.; Lambert, K.; De Muynck, D.; Vanhaecke, F.; Poelman, D.; Martins, J. C.; Allan, G.; Hens, Z. Composition and Size-Dependent Extinction Coefficient of Colloidal PbSe Quantum Dots. *Chem. Mat.* **2007**, *19*, 6101–6106.

(4)   Olkhovets, A.; Hsu, R.-C.; Lipovskii, A.; Wise, F. W. Size-Dependent Temperature Variation of the Energy Gap in Lead-Salt Quantum Dots. *Physical Review Letters* **1998**, *81*, 3539–3542.

(5)   Lhuillier, E.; Keuleyan, S.; Guyot-Sionnest, P. Optical Properties of HgTe Colloidal Quantum Dots. *Nanotechnology* **2012**, *23*, 175705.